Environ Geol (2005) 47: 1120–1127
DOI 10.1007/s00254-005-1246-x

ORIGINAL ARTICLE

Shuhab D. Khan

Urban development and flooding in Houston Texas, inferences from remote sensing data using neural network technique

Received: 27 August 2004
Accepted: 20 December 2004
Published online: 19 April 2005

S. D. Khan
Department of Geosciences,
University of Houston,
Houston, TX 77204-5007, USA
E-mail: sdkhan@mail.uh.edu
Tel.: +1-713-7433411
Fax: +1-713-7487906

Abstract The effects of urban development on the natural ecosystem and its link to the increased flooding in Houston, Texas were evaluated. Houston is suitable for this type of analysis due to its 1.95 million population, large geographic area and fast growth rate. Using neural network techniques, four Landsat Thematic Mapper images were grouped into five land use classes for the period 1984 to 2003: vegetation, bare ground, water, concrete and asphalt. Results show that asphalt and concrete increased 21% in the time period 1984–1994, 39% in 1994–2000 and 114%, from 2000 to 2003, while vegetation suffered an overall decrease. When change detection data are compared with runoff ratio data, a relationship between increased runoff and urban development is apparent, which indicates increased chances of flooding. Initial results of this work are made available to the public in GIS format via internet using Arc Internet Map Server (ArcIMS) at http://geoinfo.geosc.uh.edu/Houston.

Keywords Houston · Texas · Remote sensing · Urbanization · Flooding

Introduction

It is well documented that urbanization can have significant effects on local weather and climate (Landsberg 1981). One of the most familiar is the hydrologic impacts on streams caused by increased impervious area (e.g., roads, driveways, parking lots, and rooftops). These impacts include increased frequency of flooding and peak-flow volumes, increased sediment loading, loss of aquatic/riparian habitat, changes in stream physical characteristics (channel width and depth), decreased base flow, and increased stream temperature (Schueler 1995; Claytor and Whitney 1996).

Until recently, studies of urban effects on local landscape, ecosystem and climate were conducted for isolated locations and with in situ measurements. With the advent of high-resolution remote sensing data, it has become possible to study these effects remotely and on different scales ranging from local to global. At the present time, a considerable amount of data about the nature of the Earth's surface was collected by remote sensing devices, and the quantity is expected to increase rapidly as more images become available in the public domain, such as earth observing system (EOS) data (Asrar and Greenstone 1995). These remotely sensed data can be used to determine land-use and land-cover change detection techniques at a given point in time and land-cover changes between multiple dates (Miller et al. 1995). Given the current techniques available, remote sensing provides one of the most feasible approaches to local, regional and global land-cover change detection (Khorram et al. 1999).

Area of study

Houston, Texas is a city of 1.95 million people (US Bureau of Census 2001) with an area of approximately

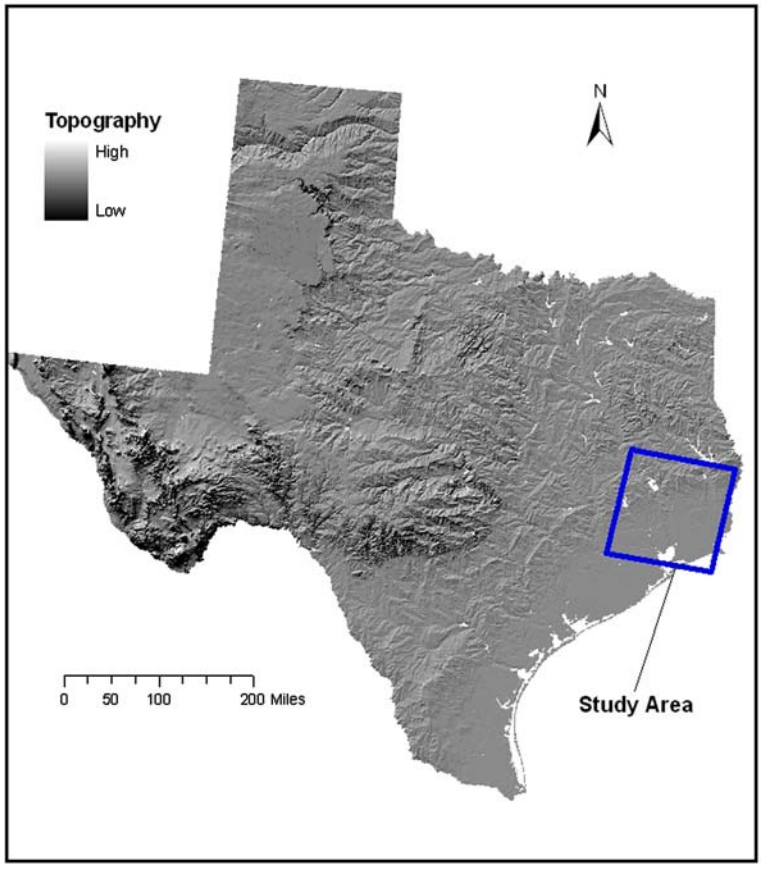

Fig. 1 Topographic map of Texas showing study area

1,400 km^2. Geographically, Houston is well suited to an analysis by remote sensing methods. A lack of city zoning laws has led to large amounts of urban sprawl, resulting in a city of large area and relatively low population density on the upper Texas Gulf Coast that lacks significant orographic features. Furthermore, Houston had undergone a period of significant growth in the last decade, including a 20% increase in inhabitants from the 1990 population of 1.63 million (US Bureau of Census 1996).

Remotely sensed change detection

For change detection, two or more registered, remotely sensed images are required that need to be obtained at different times for the same area. During the last two decades, there were many new developments in remotely sensed change detection. These techniques may be characterized by their functionalities and the data transformation procedures involved. Jensen (1996) listed several change detection algorithms, but in general, all these techniques could be classified into two groups:

1. Change Mask Development: only changes and non-changes are detected and no categorical change information can be directly provided (Examples, image differencing, image ratioing and image regression).
2. Categorical Change Extraction: complete categorical changes are extracted (examples, Normalized Difference Vegetation Index (NDVI), Tasseled Cap Transformation and Principal Component Analysis) (Lambin and Ehrlich 1996; Collins and Woodcock 1996).

Any successful remotely sensed change detection technique need to consider (1) temporal resolution, (2) spectral resolution, (3) spatial resolution and look angle, (4) radiometric resolution, (5) atmospheric conditions, (6) soil moisture conditions, (7) phenological cycle, and (8) urban–suburban phenological change

With the refinements of spatial, spectral, temporal, and radiometric resolution of sensors and faster, more efficient image processing methods, more accurate change detection can be obtained.

Materials and methods

Datasets

Satellite imageries

Four Landsat TM images were selected for path 25 and row 39 to examine changes caused by urbanization in

Table 1 Land classification using neural network technique on Landsat TM (in percentage)

Year	Asphalt	Vegetation	Water	Concrete	Bare ground
1984	2.72	75.55	10.4	1.29	10.04
1994	3.01	84.07	9.32	1.38	2.22
2000	3.88	83.28	8.22	1.54	3.07
2003	4.5	75.96	9.09	3.04	7.4

Houston area from 1984 to 2003 (Fig. 1). The data for selected scenes were acquired in 5 November 1984, 19 December 1994, 10 January 2000 and 18 January 2003. The Landsat TM sensor collects spectral data using seven bands, three in the visible portion of the electromagnetic spectrum (0.45–0.52, 0.52, 0.60, 0.63–0.69 μm); one in the near-infrared portion (0.76–0.90 μm); two in mid-infrared (1.55–1.75, 2.08–2.35 μm); and one in thermal-infrared (10.40–12.50 μm). The spatial resolution of the sensor is 30 m for visible near and mid-infrared and 120 m for thermal infrared. The temporal resolution is approximately 16 days.The use of image data from the same sensor ensures consistency in spatial, spectral, temporal, and radiometric resolution (except for variation and degradation of the sensor). Having the same spatial resolution in all images eliminates the need to resample images to a uniform pixel size. Images with

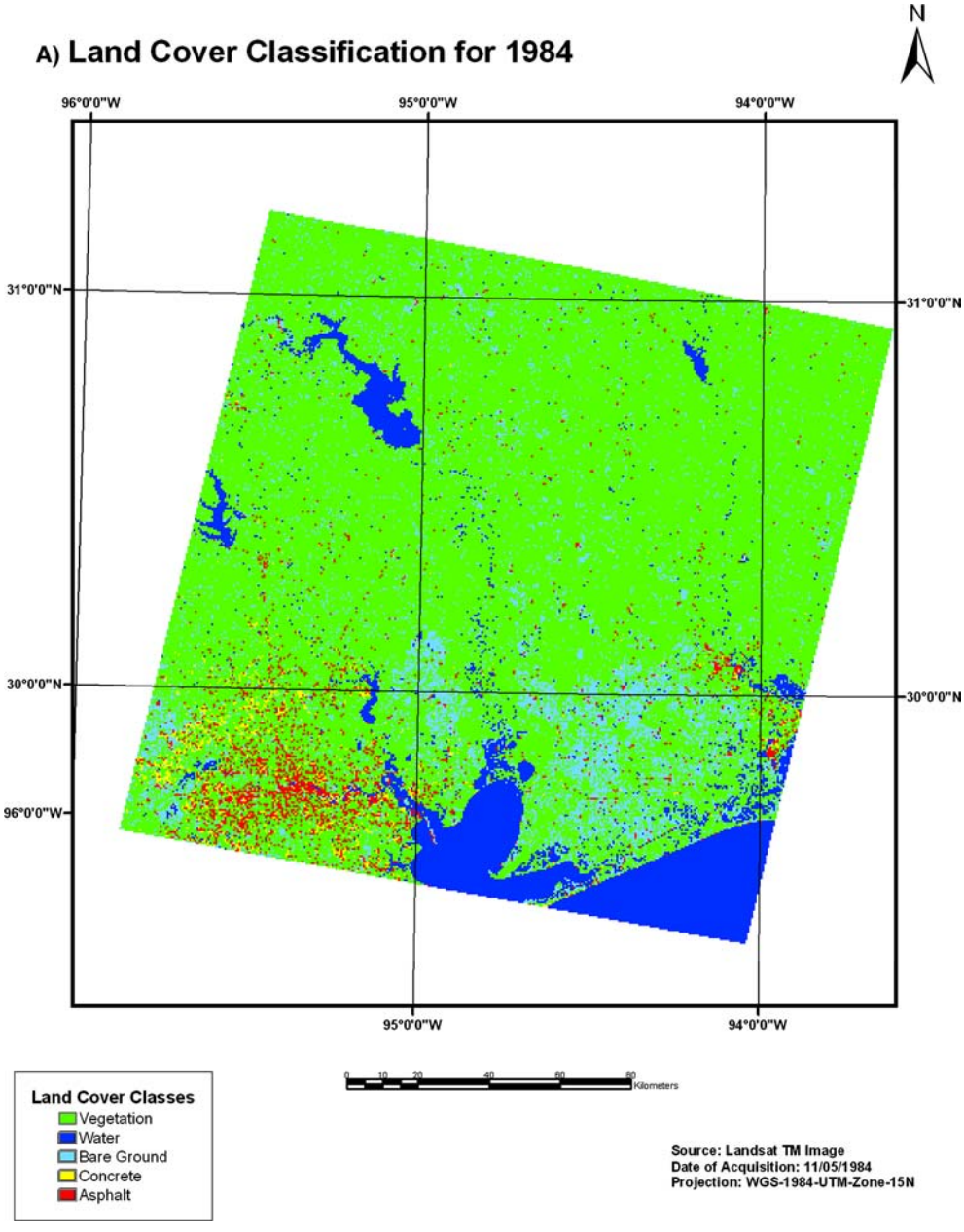

Fig. 2 Land classification using neural network technique for Houston area **a** 1984 **b** 1994 **c** 2000 **d** 2003

Fig. 2 (Contd.)

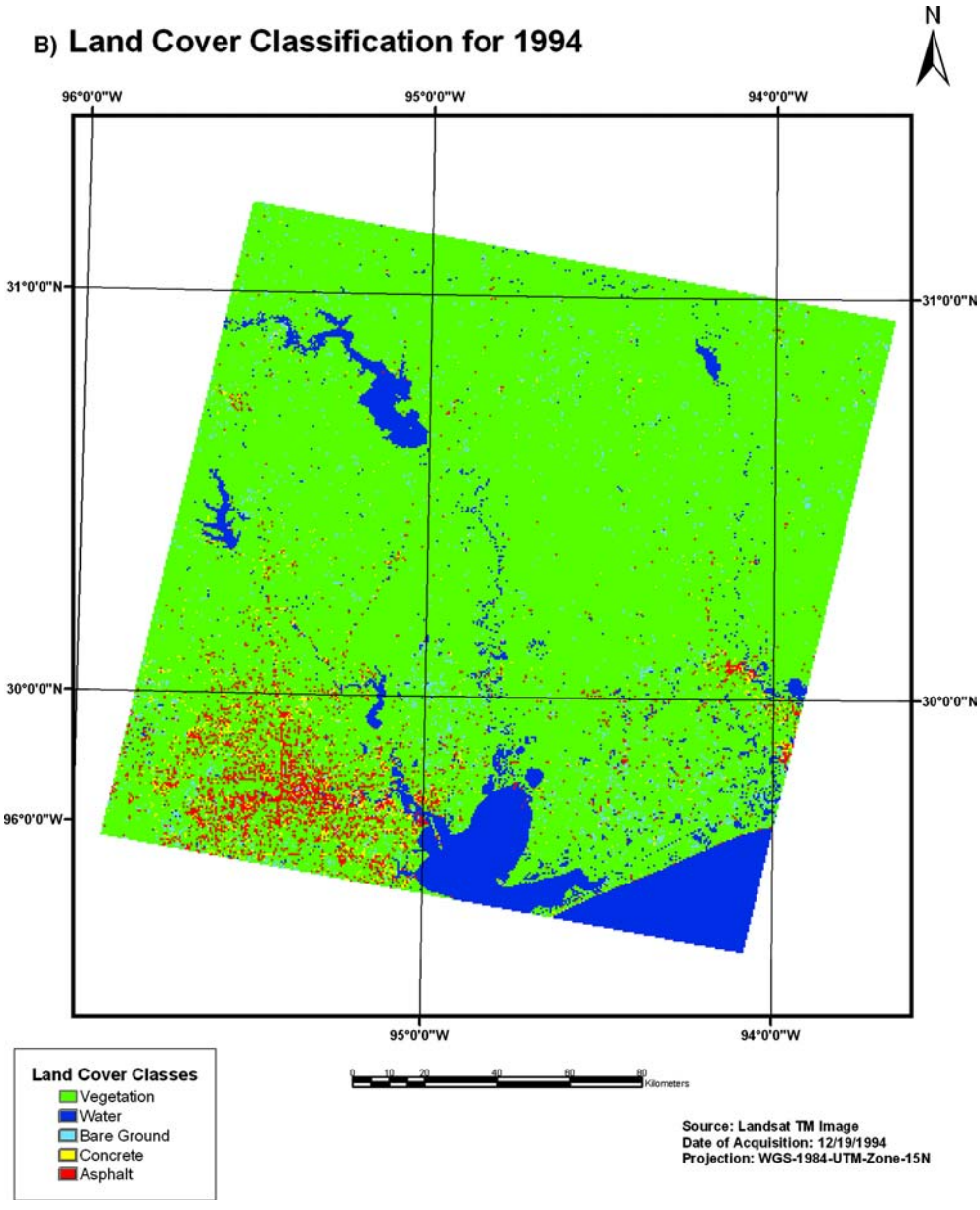

minimum cloud cover were collected in wintertime when vegetation cover and humidity were least.

Reflectance values were computed for all the Landsat TM scenes following these procedures:

1. Gain and offset parameters (Barker 1983) was applied in each band
2. The additive term was removed from each picture element for each band
3. The corrected radiance values was normalized by the solar irradiance term, integrated over the appropriate band passes.

The resultant data is proportional to surface bidirectional reflectance multiplied by an attenuation factor due to extinction of light by atmospheric absorption and scattering. No further corrections need to be made, because the relative variations of interest are largely independent of any broad wavelength dependent factors associated with atmospheric extinction. All scenes were registered to the most recent scene (acquired on 18 January 2003) using first order linear transformation with nearest neighborhood resampling method (RMS error < 15 m).

Fig. 2 (Contd.)

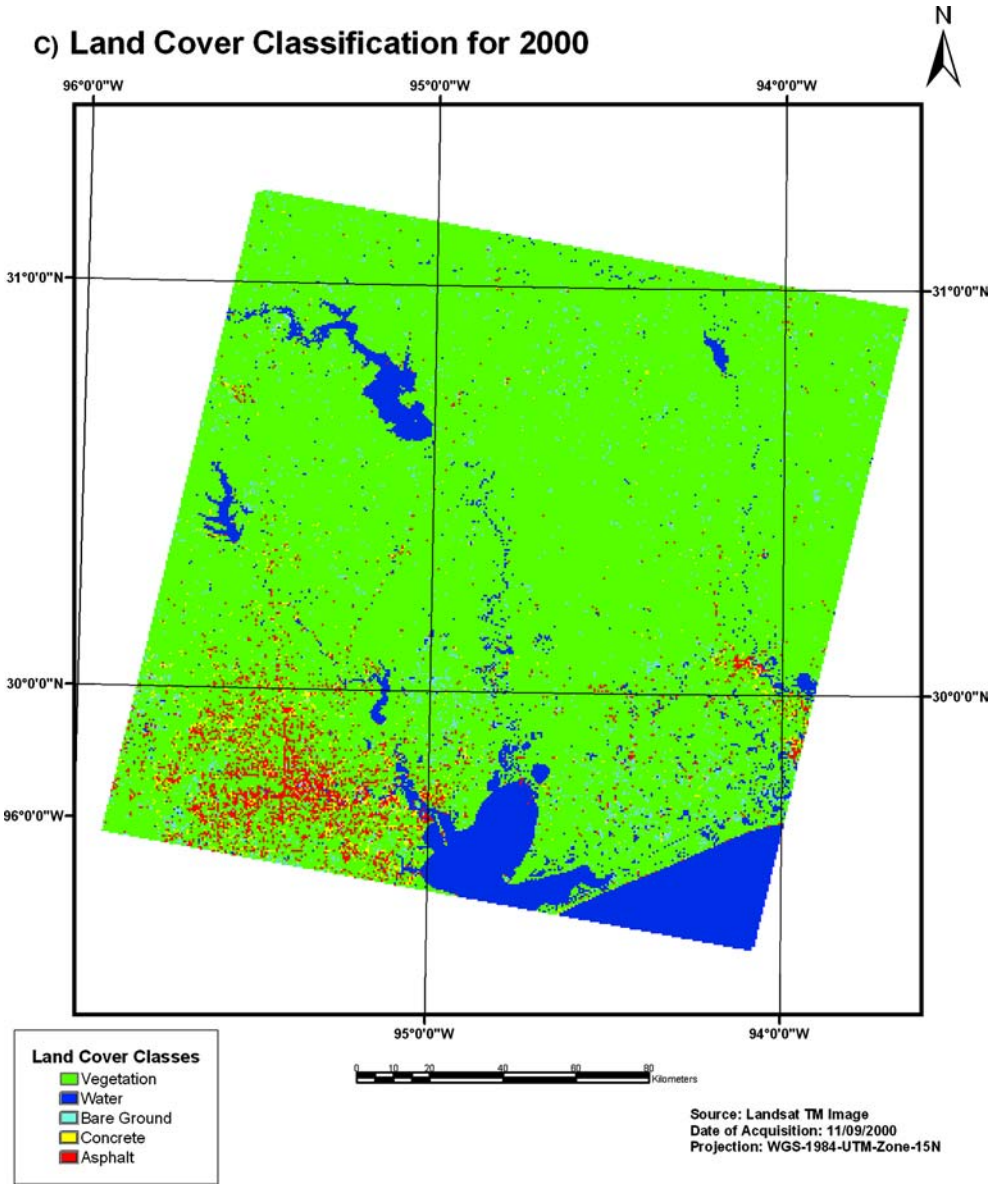

Surface runoff and precipitation data

Daily stream-flow records were obtained from a national Hydro-Climatic Data Network (HCDN) for the study area. Since 1887, the US Geological Survey (USGS) has operated a streamflow-gaging program to collect information about the Nation's water resources. Under this program, the USGS collects the streamflow data needed by Federal, State, and local agencies for planning and operating water-resources projects and regulatory programs (Wahl et al. 1995). Data were obtained from 1984 to 2003 for different sites within the study area and the cumulative runoff was calculated from 1984 to 1994 and from 1994 to 2002 for each site.

Precipitation data was obtained from Spatial Climate Analysis Service, Oregon State University (http://www.ocs.orst.edu/prism/products/)

The grid data was downloaded for each year (1944–2002). The spatial resolution for each cell is 4 km. To see the cumulative precipitation for every 10 years, the precipitation grids were then generated by summing annual grids using ArcMap. A mask that delineated the boundary of different watersheds was used to generate precipitation data for different watersheds in the study area. To determine the percentage change in precipitation for every 10 years, the change precipitation grids were generated by using a raster calculator in Arc Map.

Fig. 2 (Contd.)

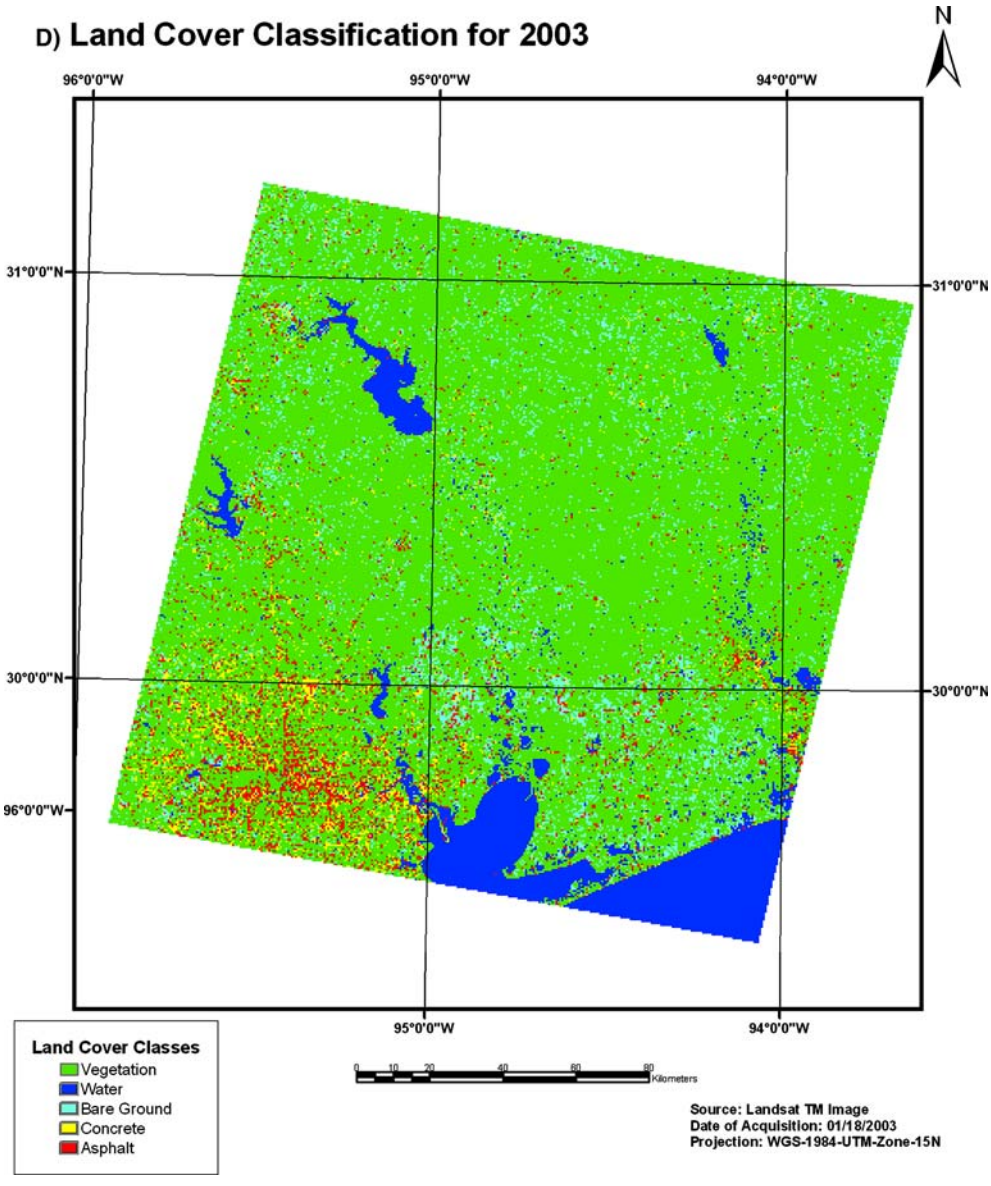

Classification

For classification and change detection of these images, a combination of post-classification and manual on-screen digitization methods was used. Post-classification comparison and manual digitization methods are described separately by Jensen (1996). The main disadvantage faced in this process was that only changes with large spectral differences were identifiable (e.g., from vegetation to urban) but small changes in land-cover types were difficult and time-consuming to detect. It was found, however, that the neural network model proved to be more useful to classify the images for different years and this technique was used. It is loosely based on the brain's nerve cell with the function of collection, processing and dissemination of electrical signals (Russell and Norvig 2003). A neural networks reaches a solution not by a step-by-step algorithm or a complex logical program, but in an unstructured fashion based on the neurons' activation function (Rao and Rao 1993). Some researchers have found superior results when classifying remote sensing data (e.g., Atkinson and Tatnall 1997; Jensen et al. 1999) by this method.

The algorithm that determines the operation of the neural network is simple:

- Weight is assigned to each input-link
- Each weight is multiplied by the input value (0 or 1)
- All the weight-firing input combinations are summed
- If sum > threshold for the neuron, then
  Output = +1
  Else output = −1

Table 2 Land cover change in the greater Houston area using Landsat TM (Unit: %). From 1984 till 2003

	Asphalt	Vegetation	Water	Concrete	Bare ground	Total
1984	2.72%	75.55%	10.40%	1.29%	10.04%	100%
1994	3.01%	84.07%	9.32%	1.38%	2.22%	100.00%
1984 (pixels)	990,264	27,532,126	3,788,861	471,785	3,658,539	36,441,575
1994 (pixels)	1,114,049	31,105,962	3,447,473	510,239	821,084	36,998,807
Change(1984–1994)	13%	13%	−9%	8%	−78%	
1994	3.01%	84.07%	9.32%	1.38%	2.22%	100.00%
2000	3.88%	83.28%	8.22%	1.54%	3.07%	100.00%
1994 (pixels)	1,114,049	31,105,962	3,447,473	510,239	821,084	36,998,807
2000 (pixels)	1,428,806	30,644,216	3,025,128	568,317	1,129,671	36,796,138
Change (1994–2000)	28%	−1%	−12%	11%	38%	
2000	3.88%	83.28%	8.22%	1.54%	3.07%	100.00%
2003	4.50%	75.96%	9.09%	3.04%	7.40%	100.00%
2000 (pixels)	1,428,806	30,644,216	3,025,128	568,317	1,129,671	36,796,138
2003 (pixels)	1,660,479	28,045,989	3,357,351	1,123,331	2,732,585	36,919,735
Change(2000–2003)	16%	−8%	11%	98%	142%	

Neural network technique was used to classify the images into five land-use classes. The five classes included vegetation, asphalt, concrete, bare ground and water and were selected based on their relevance to flooding and urbanization using a neural network technique. Results of land area ratios are summarized in Table 1. Figure 2 shows classified images for 1984, 1994, 2000 and 2003.

Change detection

The post-classification comparison change detection technique, which is the most commonly used quantitative method of change detection, was used. It requires rectification and classification of each remotely sensed image. The resulting two maps are then compared on a pixel-by-pixel basis using a change detection matrix (Jensen et al. 1993).

This technique produces a classification image which shows the differences between any pair of initial state and final state images. The difference is computed by subtracting the initial state image from the final state image (i.e., final–initial), and the classes are defined by change thresholds. For the most accurate results, the images were co-registered before processing.

Two maps of different dates were selected as initial and final states maps and from these, a change image map consisting of brightness value for each class was created. Table 2 shows the initial state classes in the

Table 3 Correlation between runoff and precipitation as runoff ratio

Site no.	Station name	Runoff ratio (1984–994)	Runoff ratio (1994–2003)
8033500	Neches Rv nr Rockland, TX	0.212	0.192
8066170	Kickapoo Ck nr Onalaska, TX	0.287	0.216
8029500	Big Cow Ck nr Newton, TX	0.321	0.247
8040600	Neches Rv nr Town Bluff, TX	0.218	0.217
8066200	Long King Ck at Livingston, TX	0.217	0.241
8066250	Trinity Rv nr Goodrich, TX	0.111	0.141
8066300	Menard Ck nr Rye, TX	0.181	0.330
8066500	Trinity Rv at Romayor, TX	0.111	0.143
8041500	Village Ck nr Kountze, TX	0.286	0.257
8070000	E Fk San Jacinto Rv nr Clevelan	0.183	0.281
8041000	Neches Rv at Evadale, TX	0.220	0.223
8070500	Caney Ck nr Splendora, TX	0.210	0.347
8068000	W Fk San Jacinto Rv nr Conroe,	0.152	0.253
8068500	Spring Ck nr Spring, TX	0.198	0.246
8041700	Pine Island Bayou nr Sour Lake,	0.375	0.321
8069000	Cypress Ck nr Westfield, TX	0.203	0.260
8076000	Greens Bayou nr Houston, TX	0.392	0.467
8075770	Hunting Bayou at IH 610, Houston	0.388	0.559
8073500	Buffalo Bayou nr Addicks, TX	0.251	0.321
8073600	Buffalo Bayou at W Belt Dr at H	0.269	0.350
8074500	Whiteoak Bayou at Houston, TX	0.432	0.503
8075000	Brays Bayou at Houston, TX	0.698	0.768
8075730	Vince Bayou at Pasadena, TX	0.442	0.661

columns and the final state classes in the rows. For each initial state class (i.e., each column), the table indicates how these pixels were classified in the final state image.

The change in pixels row indicates the total number of initial state pixels that changed classes.

Correlation between urbanization and flooding

Land cover area ratios, which were obtained from the land cover classification of the Houston area from 1984, 1994, 2000 and 2003, are shown in Table 1. Concrete and asphalt increased by about 21% from 1984 to 1994, by 39% from 1994 to 2000 and by 114% from 2000 to 2003. In contrast, vegetation increased by 13% from 1984 to 1994 but decreased by 1% from 1994 to 2000 and by 8% from 2000 to 2003. The increase in concrete and asphalt, and overall decreases in vegetation clearly show an increase in urbanization.

To estimate flooding and its relation to urbanization, the relationship between rainfall and runoff was examined by means of the runoff ratio (R/P) which is a measure of overall basin hydrologic response. Runoff ratio was calculated by using the runoff and precipitation data obtained from national databases of climate and stream flow as described earlier. Surface runoff data was converted from cubic feet per second to cubic kilometers per year and divided by the drainage basin area. Precipitation was converted to cubic kilometers, and the resulting numbers are shown in Table 3. Runoff ratio data shows overall increase in surface runoff with the exception of a few sites like site no 8033500 on the Neches River in Rockland, where the decrease in runoff can be attributed to the construction of new reservoir in the area.

Currently a web-based application is being developed, which will provide results of this work to the public via ArcIMS (ARC Internet Map Server), ArcIMS is widely utilized in the integration of local GIS data sources with internet sources for display, query, and analysis using a web browser.

Acknowledgements This work was funded by Environmental Institute of Houston. Some of the data was obtained from CSR, UT; Austin is thanked for providing Landsat dataset. Bibi Naz and Hongmei Cao are acknowledged for their help in image processing and ArcIMS web page development.

References

Asrar G, Greenstone R (1995) MTPE/EOS reference handbook, NASA/Goddard Space flight center, Greenbelt, Maryland

Atkinson PM, Tatnall ARL (1997) Neural networks in remote sensing. Int J Remote sens 18(4):699–709

Barker JL (1983) Radiometeric calibration and processing procedures for reflective bands on Landsat-4 protoflight. In: Proceedings of Landsat-4 scientific characterization early results symposium, A-23-1, NAsa/GSFC, Greenbelt, MD

Claytor RA, Whitney EB (1996) Environmental indicators to assess stormwater control programs and practices. Prepared by the Center for Watershed Protection, Silver Spring, Maryland, in cooperation with the US Environmental Protection Agency

Collins JB, Woodcock CE (1996) An assessment of several linear change detection techniques for mapping forest mortality using mutlispectral Landsat TM data. Remote Sens Environ 56:66–77

Jensen JR (1996) Introductory digital image processing a remote sensing perspective. Prentice Hall, Englewood Cliffs

Jensen JR, Narumalani S, Weatherbee O, Mackey HEM (1993) Measurement of seasonal and yearly cattail and waterlily changes using multidate SPOT Panchromatic data. Photogramm Engineering Remote Sens 59(4):519–525

Jensen JR, Qiu F, Petterson K (1999) A neural network image interpretation system to extract rural and urban land use and land cover information from remote sensor data. Geocarto Int 16(1):19–28

Khorram S, Biging GS, Chrisman NR, Colby DR, Congalton RG, Dobson JE, Ferguson RL, Goodchild MF, Jensen JR, Mace TH (1999) Accuracy assessment of remote sensing devised change detection. ASPRS Monograph, American Society for Photogrammetry and Remote Sensing, Bethada

Lambin EF, Ehrlich D (1996) The surface temperature-vegetation index space for land cover and land cover change analysis. Int J Remote Sens 17(3):463–487

Landsberg HE (1981) The urban climate. Academic, New York

Miller DM, Kaminsky EJ, Rana S (1995) Neural network classification of remote sensing data. Comput Geosci 21(3):377–386

Rao VB, Rao HV (1993) C++ neural network and fuzzy logic. Management Information, New York

Russell SJ, Norvig P (2003) Artificial intelligence: a modern approach, 2nd edn. Prentice Hall, Upper Saddle River

Schueler T (1995) Environmental land planning series: site planning for urban stream protection. Prepared by the Metropolitan Washington Council of Governments and the Center for Watershed Protection, Silver Spring, Maryland

US Bureau of Census (1996) Land area, population, and density for metropolitan areas: Population Distribution Branch, US Bureau of the Census, Washington

US Bureau of Census (2001) Land area, population, and density for metropolitan areas. Population Distribution Branch, US Bureau of the Census, Washington

Wahl KL, Thomas WO, Hirsch RM (1995) Stream-gaging program of the U.S. Geological Survey.U.S. Geological Survey Circular 1123, Reston, Virginia